



## Experimental observation of frequency doubling in a viscoelastic mixing layer

F. Sausset<sup>a</sup>, O. Cadot<sup>a,1,\*</sup>, S. Kumar<sup>b</sup>

<sup>a</sup> *Physique et mécanique des milieux hétérogènes, École supérieure de physique et de chimie industrielle,  
10, rue Vauquelin, 75231 Paris cedex, France*

<sup>b</sup> *Department of Chemical Engineering and Materials Science, University of Minnesota, 151 Amundson Hall,  
421 Washington Ave. SE, Minneapolis, MN 55455, USA*

Received 12 July 2004; accepted after revision 5 October 2004

Available online 5 November 2004

Presented by Patrick Huerre

---

### Abstract

An experimental mixing layer in water at Reynolds number 440 is investigated. A colored viscoelastic solution is introduced in the shear layer before the roll-up dynamics. On the basis of flow visualization and local velocity measurements, it is found that compared to the Newtonian case, the roll-up process is affected by the non-Newtonian behavior of the viscoelastic solution. The effect consists of the appearance of secondary eddies in the mixing layer corresponding to the production of higher harmonics in the vorticity distribution. Consequently, there is a frequency doubling of the local velocity oscillations in the mixing layer.

**To cite this article:** *F. Sausset et al., C. R. Mécanique 332 (2004).*

© 2004 Académie des sciences. Published by Elsevier SAS. All rights reserved.

### Résumé

**Observation expérimentale de doublement de fréquence dans la couche de mélange viscoélastique.** Une étude expérimentale de la couche de mélange à un nombre de Reynolds de 440 est réalisée. Une solution viscoélastique colorée est introduite dans la couche cisaillée stationnaire juste avant la formation des tourbillons. En utilisant une mesure locale de la vitesse et une technique de visualisation par fluorescence, il est montré que la formation tourbillonnaire est affectée par le comportement non-Newtonien de la solution viscoélastique par rapport au cas Newtonien. Cet effet correspond à la formation de tourbillons secondaires produisant un harmonique supérieur dans la répartition spatiale de vortacité. En conséquence, un doublement de la fréquence des oscillations de la vitesse locale dans la couche de mélange est observé. **Pour citer cet article :** *F. Sausset et al., C. R. Mécanique 332 (2004).*

© 2004 Académie des sciences. Published by Elsevier SAS. All rights reserved.

---

\* Corresponding author.

*E-mail addresses:* [sausset@rip.ens-cachan.fr](mailto:sausset@rip.ens-cachan.fr) (F. Sausset), [cadot@ensta.fr](mailto:cadot@ensta.fr) (O. Cadot), [kumar@cems.umn.edu](mailto:kumar@cems.umn.edu) (S. Kumar).

<sup>1</sup> Present address: Unité de mécanique de l'École nationale supérieure de techniques avancées, chemin de la Hunière, 91761 Palaiseau cedex, France.

*Keywords:* Fluid mechanics; Mixing layer; Elasticity; Harmonic production

*Mots-clés :* Mécanique des fluides ; Couche de mélange ; Élasticité ; Production d'harmoniques

## Version française abrégée

La couche de mélange est un ingrédient essentiel pour les écoulements naturels et industriels mettant en jeu des cisaillements turbulents éloignés des parois. Depuis les premières études [1,2], la dynamique de la couche de mélange ainsi que les structures cohérentes qu'elle produit ont été abondamment étudiées dans le cas des fluides Newtoniens. Cependant sa contre-partie en fluides non-Newtoniens a été comparativement peu étudiée. Théoriquement et numériquement, l'élasticité est connue pour stabiliser l'instabilité de Kelvin–Helmholtz [3–6]. A part quelques études de couches de mélanges turbulentes avec additifs de polymères [9,10], nous ne connaissons pas d'expériences qui s'intéressent aux effets viscoélastiques sur la couche de mélange laminaire. Dans le présent travail, la couche de mélange est produite dans un tunnel hydrodynamique (écoulement à vitesse  $U = 8$  cm/s) par une marche descendante (cf. Fig. 1(a)). Le fluide dans le tunnel est de l'eau ; une solution de liquide viscoélastique est introduite dans la couche limite (avant la marche) par une injection au travers de 60 trous (cf. Fig. 1(a)). Le liquide viscoélastique est une solution de Poly Oxyde Ethylène (PEO) de masse molaire  $9 \times 10^6$  g/mol et concentrée à 2000 ppm dans de l'eau. La viscosité de cisaillement de la solution est montrée en Fig. 1(b), on y voit un grand effet d'amincissement de cisaillement où le plus grand temps de relaxation  $\tau = 0,9$  s est estimé avec le modèle de Carreau. L'épaisseur initiale des couches de mélange  $\delta_0$  est estimée à partir du champ de vitesse de l'écoulement moyen (cf. Fig. 2). Les nombres de Reynolds, de Weissenberg et l'Elasticité sont estimés en Éq. 2. Du point de vue de la dynamique, les deux couches de mélange ont des comportements différents comme le montrent les deux séries temporelles de la vitesse locale (cf. Fig. 3(a)) effectuées à l'aide d'une sonde acoustique pour chacune des deux injections. Le cas d'injection de solution de PEO, présente plus d'oscillations que le cas Newtonien. En fait, les spectres d'amplitudes (cf. Fig. 3(b)) des signaux de vitesses nous montrent que le pic fondamental est observé aux alentours de  $f = 0,8$  Hz dans les deux cas Newtoniens (avec et sans injection d'eau) avec un premier harmonique de faible amplitude. Pour le cas non-Newtonien, on trouve d'une part que le pic fondamental est légèrement décalé vers les basses fréquences et d'autre part que le premier harmonique est d'amplitude comparable au fondamental. On observe donc un doublement de la fréquence locale dans la couche de mélange en présence de liquide viscoélastique. Les visualisations de l'écoulement nous dévoilent que souvent, la formation d'un tourbillon dans la couche de mélange s'accompagne par la formation d'un second tourbillon (cf. Fig. 4). Ce sont ces paires de tourbillons qui sont à l'origine du doublement de fréquence. Le décalage du fondamental vers les basses fréquences est cohérent avec les prédictions théoriques de la stabilisation de la couche de mélange par l'élasticité dans le régime linéaire. L'apparition du premier harmonique est sans doute en relation avec la simulation numérique de Kumar et Homsy [6] qui révèle la production d'une harmonique de la distribution de la vorticit  pendant la formation des tourbillons. Il en résulte l'apparition de deux tourbillons au lieu d'un seul. Cet effet n'avait encore jamais été observé expérimentalement. A l'avenir, nous désirons développer l'analogie qui existe entre effets de tension de surface et effets viscoélastiques sur l'instabilité de Kelvin–Helmholtz [3,8]. En effet, dans le cas Newtonien et pendant le régime non linéaire de l'instabilité, la tension de surface est aussi à l'origine de production d'harmoniques [7] pendant le processus de concentration de la vorticit .

## 1. Introduction

The mixing layer is an essential ingredient in natural and industrial flows involving turbulent free shear layers. Since primary works [1,2], coherent structures such as spanwise vortices resulting from the Kelvin–Helmholtz instability and the subsequent streamwise vortices have been the subject of extensive studies. On the other hand, its

non-Newtonian counterpart has been poorly studied experimentally. Numerically and theoretically, the presence of elasticity is known to stabilize the Kelvin–Helmholtz instability [3], slowing down the roll-up process and shifting the most unstable wavenumber to smaller values. The 3D mechanism for the formation of the streamwise vortices is also found to be inhibited by the elasticity [4,5]. In the numerical simulation of Kumar and Homay [6], a scenario of the 2D stabilization mechanism is identified. The simulation reveals a higher harmonic production of the vorticity during the roll-up process. The higher harmonics resist the tendency of the fundamental to concentrate the vorticity into a single core region. The large polymer stress gradients are responsible for this effect. Similarly, a kind of higher vorticity harmonic production is also found during the roll-up dynamics of a vorticity sheet with surface tension [7]. The analogy between surface tension and the polymer stress was pointed out by Hinch in an appendix to [3] and successfully applied to understand the topology of the viscoelastic wake of a cylinder [8]. While flow visualization shows the strong effects of polymer additives on the turbulent mixing layer [9,10], few experiments study viscoelastic effects on laminar instabilities in the mixing layer.

In the present experiment, we investigate the viscoelastic mixing layer at moderate Reynolds numbers. One component of the local velocity is measured with an acoustic Doppler anemometer and the results are illustrated with flow visualization by laser induced fluorescence. The aim of this article is to announce a preliminary but significant result about the effect of polymers on the non-linear development of the Kelvin–Helmholtz instability.

## 2. Experimental set-up

The flow is produced in a water tunnel. The experimental geometry is shown in Fig. 1(a). The velocity of the main flow is  $U = 8$  cm/s. The boundary layer that develops on the bottom of the tunnel is suddenly subjected to a large backward facing step at  $x = 0$  cm of height  $h = 10$  cm equal to the height the tunnel was before the step (for  $x < 0$  cm). After the step, the velocity profile has an inflexion point (see displayed velocity profiles in Fig. 1(a)), which is the origin of the Kelvin–Helmholtz instability.

As in the experiments in [5] or [8], the main flow is Newtonian (water only). Either dyed viscoelastic solution or dyed water is introduced before the backward facing step, in the stationary shear layer, through 50 holes of 0.7 mm in diameter located at  $x = -5$  cm (see Fig. 1(a)). The apparatus used to control the injection rate is the same as the one used in [5] or [8]. We define the injection rate parameter  $\beta = u/U$  as the ratio of the velocity at the exit of the holes,  $u$ , to the main velocity,  $U$ . For the present experiment,  $\beta = 0.3$  and remains unchanged. We studied both the cases where either the viscoelastic solution or water is injected. We also compare the water injection case to the

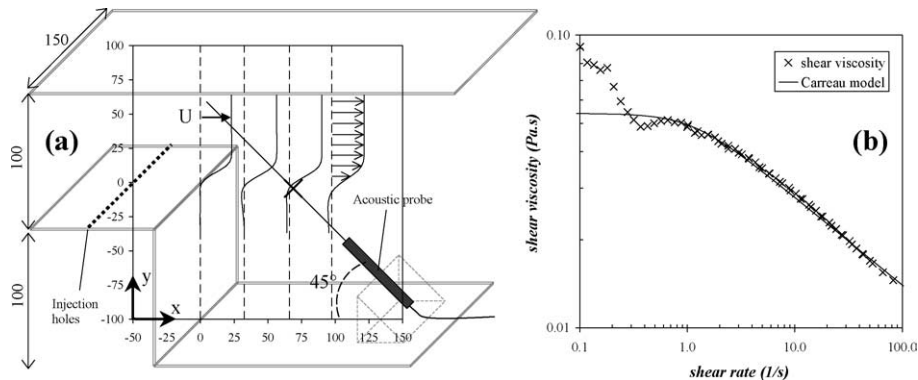


Fig. 1. (a) Experimental set-up; distances are in mm. The  $x$ -velocity profiles of the mean Newtonian flow show the development of the mixing layer. The acoustic anemometer is used to obtain time series of the velocity component along the probe axis at the location which is shown by the bold cross. (b) Shear viscosity of the PEO solution measured with a constant shear rate rheometer from Stress Tech. The solid line is the fit of the Carreau model,  $\eta = \eta_0(1 + (\tau\dot{\gamma})^2)^{-N}$ , where  $\eta_0 = 54 \times 10^{-3}$  Pa s,  $\tau = 0.9$  s, and  $N = -0.15$ .

case without any injection at all in order to estimate the disturbance of the boundary layer due to the injection. The viscoelastic solution we use is Poly Ethylene Oxide having  $9 \times 10^6$  g/mol molecular weight and concentrated at 2000 wppm in water. The shear viscosity displayed in Fig. 1(b) exhibits a strong shear thinning behaviour, and the largest relaxation time of the solution  $\tau = 0.9$  s is estimated with the Carreau model.

The velocity of the mean flow is measured by a PIV technique from Lavision. The laser sheet is in the  $(x, y)$  plane and located in the symmetry plane of the tunnel; a resulting velocity field is displayed in Fig. 1(a). The temporal resolution of our PIV set-up (corresponding to a sampling rate of 4 Hz) is not sufficient to capture the roll-up dynamics of the mixing layer. We then use an acoustic Doppler anemometer (DOP 1000 from Signal Processing SA) having a sampling frequency of 30 Hz and measuring one component of the velocity along the probe axis. A crucial advantage of this velocity measurement is that it is independent of the rheology of the solution (which is not the case for hot film anemometry). On the other hand the spatial resolution is rather poor ( $8 \text{ mm} \times 8 \text{ mm}$ ), which is not a limitation for the present application since we are interested in the temporal evolution.

### 3. Results

We first present the effect of the injection on the mean flow. The  $x$ -velocity profiles,  $U_x(x, y)$ , are measured with a PIV technique over 60 fields taken with a sampling frequency of 4 Hz. Both the cases of water injection and polymer solution injection are superimposed in Fig. 2(a). Differences between the two cases are hardly distinguishable. From these profiles, we estimate a local vorticity thickness that we define as:

$$\delta^2(x) = \frac{\int y^2 (dU_x(x, y)/dy) dy}{\int (dU_x(x, y)/dy) dy} \quad (1)$$

The spatial evolution of the thickness  $\delta(x)$  for both injection cases shown in Fig. 2(b) is very similar:  $\delta$  increases due to viscous diffusion and momentum convection. At the beginning of the mixing layer ( $x = 0$  cm in Fig. 2(a)), the thicknesses for both cases are close to  $\delta_0 = 5.5$  mm. We can notice that the thickness is smaller for polymer injection except for larger distances, after  $x = 7$  cm, where it becomes larger than with water. The vorticity thickness and the largest relaxation time of the solution allow us to compute dimensionless numbers such as the Reynolds number, the Weissenberg number, and the elasticity number using similar definitions to those introduced in [5]:

$$Re = \frac{U \delta_0}{\nu} = 440; \quad We = \frac{\tau U}{\delta_0} = 14, \quad E = \frac{We}{Re^*} = \frac{\tau \nu_p}{\delta_0^2} = 0.74 \quad (2)$$

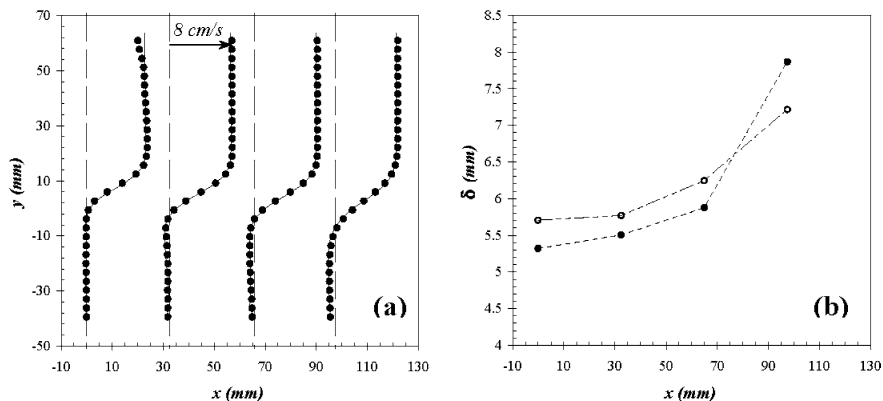


Fig. 2. (a)  $x$ -velocity profiles. The black filled circles are the measurements when the PEO solution is injected, and the continuous line is for water injection. (b) Vorticity thickness,  $\delta(x)$ , deduced from each mean velocity profile (see definition in Eq. (1)) for water injection (empty circles) and PEO solution injection (black filled circles).

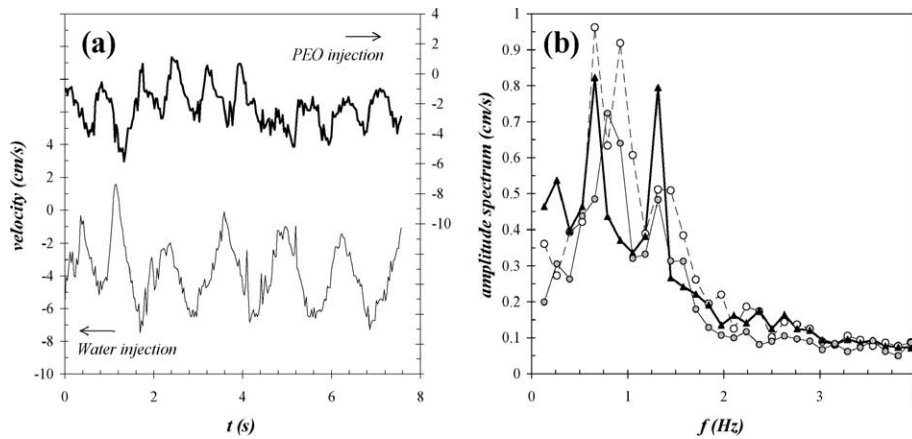


Fig. 3. (a) Time series of the local velocity measured with the Doppler acoustic anemometer with water injection (thin line) and with PEO solution injection (thick line). (b) Amplitude spectra of the time series with no injection (grey symbols), water injection (empty symbols), and PEO solution injection (black symbols).

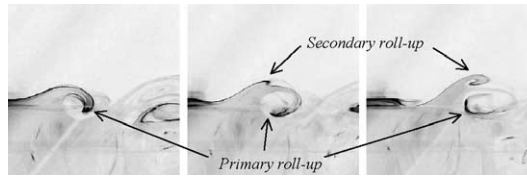


Fig. 4. Video picture sequence of the secondary roll-up process. The time duration between two consecutive pictures is 0.33 s and the picture size is 8 cm  $\times$  8 cm.

Since the mixing layers with and without polymers are rather similar, we are tempted to take the water kinematic viscosity for a definition of the Reynolds number relevant to the global description of the flow dynamics. However, in the viscoelastic solution, the shear kinematic viscosity is much larger than that for water. The shear viscosity can be estimated from Fig. 1(b), taking  $U/\delta_0 = 14.5 \text{ s}^{-1}$  as the typical shear rate of the mixing layer. For this shear rate, the shear viscosity is  $\nu_p = 25\nu$  and the local Reynolds number is  $Re^* = U\delta_0/\nu_p$ . The elasticity number relevant to polymer effects should be based on the Weissenberg number and the corrected Reynolds number  $Re^*$ .

In Fig. 3(a), we show an 8 s sample of the time series of one component of the velocity extracted from the acoustic anemometer measurements. The component corresponds to the projection of the velocity vector at the cross location (see Fig. 1(a)) on the probe axis (oriented  $45^\circ$  from the  $x$ -axis). On this sample, the difference between both injection cases is striking: the frequency of the velocity fluctuations is much larger for injection of viscoelastic solution than for injection of water. We calculate amplitude spectra of the velocity fluctuations over a time duration of 190 s; these are displayed in Fig. 3(b). We also show the spectrum for the undisturbed mixing layer (grey symbols, no injection). In this case, a fundamental peak is observable around  $f = 0.8 \text{ Hz}$ . The injection of water seems to enlarge this peak while the injection of polymer solution drastically changes the spectrum. The fundamental peak is slightly shifted to smaller frequencies and an harmonic of comparable amplitude appears. Both peaks are also thinner than the fundamental peak observed for the Newtonian case. This observation implies that the viscoelastic flow is the most periodic flow. We visualize the flow by coloring the solutions with a fluorescent dye. We observe that for the viscoelastic flow, eddies that are being formed by the roll-up of the mixing layer are often accompanied by a secondary roll-up process. The typical scenario is shown by the video sequence in Fig. 4 where the viscoelastic solution appears black.

#### 4. Discussion and conclusion

Our experiment shows that viscoelastic solution in the mixing layer affects the dynamics of the vortex-sheet roll-up. We found that secondary vortices are often created, causing a harmonic production of vorticity. Such a mechanism has never been reported before in experiments. We believe this effect to be related to the mechanism observed in the numerical computation of [6]. The Weissenberg, Reynolds, and elasticity numbers of the present experiment are similar to those of the numerical computation. The viscoelastic effect seems different from the typical stabilization mechanism that consists of the inhibition of inertial instability (roll-up process) by the elasticity which usually results in an increase of the wavelength and a decrease in the growth rate [3,5]. However, these effects belong to the linear regime of the instability, when the development time of the instability is short. For the present experimental mixing layer, relatively long development times are considered and a fully non-linear mechanism is observed. However, the slight shift of the fundamental frequency to smaller values that is observed with polymers (Fig. 3(b)) is possibly related to the linear stabilization mechanism.

In the future, we will perform systematic measurements with the PIV technique for different elasticity numbers varying the shear thickness, the relaxation time of the solution, and the injection rate. We also plan to explore the 3D structure of the viscoelastic mixing layer in order to compare to the recent extensive computational study of Z. Yu and N. Phan-Thien [4].

#### Acknowledgements

We thank J. Hinch for his critical reading of the manuscript. We are grateful to D. Bonn for providing the rheometer. This work has been initialized during a stage of the cursus Phytém of ENS Cachan.

#### References

- [1] C.D. Winant, F.K. Browand, Vortex pairing: the mechanism of turbulent mixing layer growth at moderate Reynolds number, *J. Fluid Mech.* 63 (1974) 237–255.
- [2] L.P. Bernal, A. Roshko, Streamwise vortex structure in plane mixing layers, *J. Fluid Mech.* 170 (1986) 499–525.
- [3] J. Azaiez, G.M. Homsy, Linear stability of free shear flow of viscoelastic liquids, *J. Fluid Mech.* 268 (1994) 37–69.
- [4] Z. Yu, N. Phan-Thien, Linear three dimensional roll-up of a viscoelastic mixing layer, *J. Fluid Mech.* 500 (2003) 29–53.
- [5] O. Cadot, S. Kumar, Experimental characterization of viscoelastic effects on two- and three-dimensional shear instabilities, *J. Fluid Mech.* 416 (2000) 151–171.
- [6] S. Kumar, G.M. Homsy, Direct numerical simulation of hydrodynamic instabilities in two- and three-dimensional viscoelastic free shear layers, *J. Non-Newtonian Fluid Mech.* 83 (1994) 251–276.
- [7] R. Rangel, W. Sirignano, Non-linear growth of the Kelvin–Helmholtz instability; Effect of surface tension and density ratio, *Phys. Fluids* 31 (1988) 1845–1855.
- [8] O. Cadot, Partial roll-up of a viscoelastic Kármán street, *Eur. J. Mech. B Fluids* 20 (2001) 145–153.
- [9] S. Riediger, Influence of drag reducing additives on a plane mixing layer, in: R.H.J. Sellin, R.T. Moses (Eds.), *Drag Reduction in Fluid Flows*, Ellis Horwood, Chichester, England, 1989.
- [10] M. Hibberd, M. Kwade, R. Scharf, Influence of drag reducing additives on the structure of turbulence in a mixing layer, *Rheol. Acta* 21 (1982) 582–586.